Investigation of magnetic properties for Fe - Ni - P - B nanosize amorphous alloy powders prepared by chemical reduction

1996 J. Phys.: Condens. Matter 8 5451

(http://iopscience.iop.org/0953-8984/8/29/018)

J. Phys.: Condens. Matter **8** (1996) 5451–5459. Printed in the UK

Investigation of magnetic properties for Fe–Ni–P–B nanosize amorphous alloy powders prepared by chemical reduction

Zhang Bangwei†‡ and Yi Ge‡

† International Centre for Materials Physics, Academia Sinica, 110015 Shengyang, People's Republic of China

‡ Department of Applied Physics, Hunan University, Changsha 410082, People's Republic of China

Received 19 December 1995, in final form 1 April 1996

Abstract. Quaternary Fe–Ni–P–B nanosize amorphous alloy powders were prepared successfully by chemical reduction. The nanosize powders had a diameter in the range 20–200 nm. The magnetic properties were studied. The saturation magnetization of the alloy powders decreased with increasing nickel or iron in the iron-based or nickel-based alloys, respectively, which meant that there was a minimum for the magnetization versus Fe content plot. On the contrary, the coercivity of the alloy powders increased with increasing nickel or iron in the iron-based or nickel-based alloys, respectively, that is to say there was a maximum for the coercivity versus Ni content plot. The dependences of the saturation magnetization and coercivity of the alloy powders on annealing temperature were studied. It was also found that the remanence-to-saturation ratio was not larger than 0.15 even after heat treatment.

1. Introduction

Studies on nanosize amorphous alloy powders (NSAAPs) prepared by chemical reduction have recently attracted increasing attention since 1985 [1, 2]. The magnetic properties of nanosize powders can be different from those of bulk samples. For example, the coercivity H_c of bulk $Fe_{80}B_{20}$ alloys is less than 5 Oe [3] compared with approximately 1200 Oe for Fe–B nanosize powders [4]. This is also the case for Fe. The coercivity H_c of bulk Fe is only 50 Oe compared with 1540 Oe for fine powders [5]. However, this difference between the saturation magnetizations M_s of the bulk and fine powder materials is small instead of very large. The saturation magnetizations M_s of $Fe_{80}B_{20}$ and $Fe_{20}Ni_{60}B_{20}$ ribbons prepared by liquid quenching are 160 emu g^{-1} and 58 emu g^{-1} [6] compared with 125 emu g^{-1} and 60 emu g^{-1} for $Fe_{93}B_7$ and $Fe_{20}Ni_{60}B_{20}$ fine powders [7], respectively. Therefore, studies on the magnetic properties of NSAAPs are very interesting and important whether from a scientific or a technological point of view.

We have prepared the quaternary Fe–Ni–P–B NSAAPs by chemical reduction and reported their preparation conditions, crystallization and thermal properties [8–10]. In this work, we present the results of magnetic properties of the quaternary as-prepared Fe–Ni–P–B NSAAPs. To clarify how the magnetic properties of the NSAAPs are influenced by annealing, their temperature dependences are also reported.

0953-8984/96/295451+09$19.50

2. Experimental procedures

KBH_4 was used as a reduction agent. A 0.3 M KBH_4 aqueous solution was added to a mixed solution which contains 0.1 M NaH_2PO_2 and 0.2 M Fe and Ni metal ions in air with vigorous stirring. The metallic salts used were Fe and Ni sulphates. The Ni^{2+}-to-($Ni^{2+} + Fe^{2+}$) ratio ranged from 0.05 to 0.95. The powders were prepared at room temperature. The black precipitate was washed with deionized water, collected on a filter and dried in a vacuum dryer (10^{-2} Torr) at 85 °C for 3 h. The alloy composition of the powders was determined by chemical analysis. The morphology and structure of the product were examined using an H800 electron microscope and Siemens D5000 diffractometer with Cu Kα radiation. Annealing of the samples was performed in an argon atmosphere at different temperatures for 1 h. The magnetic properties for the as-prepared samples and the samples after annealing were measured at room temperature with a 9500 vibrating-sample magnetometer.

3. Results and discussion

3.1. Composition and structure

Six samples of Fe–Ni–P–B NSAAP (samples 1–6) were prepared by changing the Ni^{2+}-to-($Ni^{2+} + Fe^{2+}$) ratio from 0.05 to 0.95. Table 1 shows the alloy compositions of the samples. These compositions have been normalized to a total of 100%. The unknown fraction was 7–17 wt% for samples 1, 2, 3 and 6, but up to 35 wt% for samples 4 and 5 and was most probably oxygen. Other workers [7, 11–13] have reported that up to 40 at.% oxygen existed in their powder samples obtained by chemical reduction. It seems that oxide cannot be excluded in the precipitate using chemical reduction if contact with atmosphere is not avoided.

Table 1. Composition of Fe–Ni–P–B NSAAPs.

Sample	$Ni^{2+}/(Ni^{2+} + Fe^{2+})$ ratio	Fe (at.%)	Ni (at.%)	P (at.%)	B (at.%)
1	0.05	74.5	2.2	2.9	20.4
2	0.15	76.9	6.2	2.0	14.9
3	0.30	54.4	18.0	4.9	22.7
4	0.50	28.5	20.1	12.8	38.6
5	0.70	20.1	35.9	12.7	31.3
6	0.95	4.9	62.3	7.8	25.0

The reproducibility of sample preparation was studied by measuring the composition for the same sample prepared using different times. It has been found that the reproducibility was fairly good.

The XRD patterns of the samples show they are all typical amorphous structures. However, from the electron bright-field images and electron diffraction patterns it has been found that four samples (samples 1–3 and 6) show amorphous features and the other two samples (samples 4 and 5) show somewhat distinct contrast, revealing the existence of small crystalline phases in the halo rings. It has also been found that the amorphous powder has a spherical morphology with diameter ranging from 20 to 200 nm.

3.2. Saturation magnetization

Figure 1 shows the saturation magnetization M_s measured at room temperature versus Fe content of the six as-prepared NSAAP samples. It can be seen from the figure that M_s decreases rapidly from 121.46 to 1.84 emu g^{-1} on decreasing the Fe content from 74.47 to 20.14 at.% for the iron-based alloy and then increases slightly from 1.84 to 5.01 emu g^{-1} on increasing the nickel content from 35.84 to 62.31 at.% for the nickel-based alloy. There is a minimum in the magnetization versus composition plot. A similar compositional dependence was reported for M_s for $(Fe_{1-x}Co_x)_{63}B_{37}$ amorphous alloy powders obtained by chemical reduction [14], for which the only explanation given was that the compositional dependence for M_s was presumed to reflect the difference between the magnetic moments of iron and cobalt.

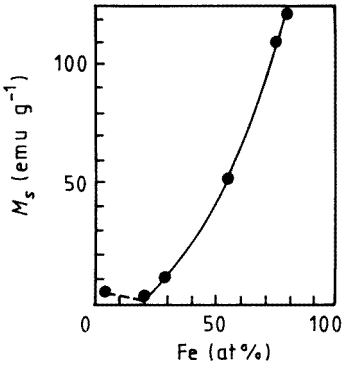

Figure 1. Saturation magnetization M_s of Fe–Ni–P–B NSAAPs as a function of Fe content at room temperature.

In the literature, many experimental data (see the review papers and books in [15–17]) have been reported on the saturation magnetization M_s of transition metal–metalliod (TM–M) glasses. For most TM–M glasses the average value of magnetic moment $\overline{\mu}$ per TM atom and therefore the M_s of the glasses decrease with increasing M content. Usually, the data have been explained on the basis of a charge-transfer (CT) model which is in fact a form of the rigid-band theory for crystalline alloy. The macroscopic atom model of Miedema and co-workers [18] is also a CT model and can give a quantitative estimate of CT. Here we refer only to the usual CT model, i.e. the rigid-band model in the discussion. According to this model the decrease in $\overline{\mu}$ is uniquely related to the numbers of s and p electrons transferred from the M atoms to the common d band of the TM atoms, but the number of transferred electrons for a given M atom is not universal and depends upon the TM–M system studied when the experimental data are explained using the model [15]. Similarly, the present data of compositional dependence of M_s for Fe–Ni–P–B NSAAPs could be understood by assuming that the numbers of electrons transferred from each phosphorus and boron atoms are $2.5\mu_B$ and $1.0\mu_B$ respectively. That is, the average value of magnetic moment $\overline{\mu}$ per Fe or Ni atom for Fe–Ni–P–B NSAAPs can be written as

$$\overline{\mu} = 2.2a + 0.6b - 2.5x - 1.0y \tag{1}$$

where a, b, x and y are the Fe, Ni, P and B contents, respectively, and $2.2\mu_B$ and $0.6\mu_B$ are the magnetic moments of pure iron and nickel atoms, respectively. The calculated results of $\overline{\mu}$ for the alloys from the above equation are shown in table 2, which indicates that the trend

for calculating the compositional dependence of $\overline{\mu}$ is similar to that of M_s. Obviously, this explanation is only a mere formality because of the following reasons for the CT model.

Table 2. Calculated average values of magnetic moment per metallic atom for Fe–Ni–P–B NSAAPs.

	1	2	3	4	5	6
$\overline{\mu}$ (μ_B)	1.38	1.53	0.96	0.042	0.027	0.037

Why are the numbers of transferred electrons from an M atom to a metallic TM atom different for various systems? The CT model cannot explain this theoretically. More seriously, modern band-structure calculations and various photoemission experiments probing the electronic structure directly show that the bands in crystalline materials are not rigid even for the simplest cases [19–22]. It is therefore expected that the rigid-band theory fails for amorphous alloys [22]. That is to say the CT model is not a realistic description of the TM–M glasses and their magnetic properties. Instead of using the CT model, a covalent bonding model is used to describe the magnetic properties of the TM–M glasses [23]. According to the covalent bonding model, the states of two atoms hybridize with one another to form bonding and antibonding hybrids when the atoms combine together. The hybridization of d states of TM atoms and sp states of M atoms forms the covalent bond in the TM–M glasses. There is no net electron transfer because the electrons in the hybrids are shared between the atoms. The result of the d–sp hybridization is a delocalization of some of the magnetic d states, and in consequence a reduction in the magnetic moment. Obviously, the more M atoms there are, the greater is the hybridization, and thereby the greater is the reduction in magnetic moment. In addition, the magnetic moment would be reduced on decreasing the Fe content. The reasons why M_s of sample 6 is greater than that of sample 5 are the amount of M atoms, i.e. there are much fewer P + B atoms for sample 6 than for sample 5; therefore, on the one hand, the hybridization and the reduction in magnetic moment of sample 6 are less than for sample 5 and, on the other hand, the magnetic moment for sample 6 is larger than that of sample 5 because the Ni concentration in sample 6 is much higher than in sample 5. In this way, the present compositional dependence of magnetization could be explained by the covalent bonding model qualitatively at least.

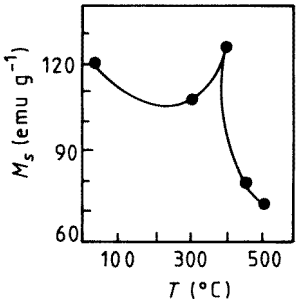

Figure 2. Temperature dependence of M_s for the sample 2 ($Fe_{76.9}Ni_{6.2}P_{2.0}B_{14.9}$).

Figure 2 shows the temperature dependence of room-temperature saturation magnetization M_s for sample 2, $Fe_{76.9}Ni_{6.2}P_{2.0}B_{14.9}$. It can be seen that, for a low annealing temperature (300 °C for 1 h), the magnetization is only slightly less than for the as-prepared

sample; then it increases to the original value again (400 °C for 1 h) and decreases sharply for an annealing temperature higher than 450 °C for 1 h. For a metallic glass ribbon prepared by splat quenching, Hatta *et al* [24] reported that the magnetization of $Fe_{84}B_{10}C_6$ alloy after isochronal (1 h) annealing showed a maximum at around 250 °C. Obviously, this is a similar result to that in the present case.

Our crystallization results on $Fe_{76.9}Ni_{6.2}P_{2.0}B_{14.9}$ NSAAPs showed that, after annealing at 300 °C for 1 h, only a small amount of α-Fe phase in the amorphous matrix could be detected by XRD and, after annealing at 400 °C for 1 h, more α-Fe phase appears but no other phases in the amorphous matrix could be detected [9]. At any temperature, two factors will affect M_s; however, they operate in opposite directions. One is the compositional short-range ordering caused by structural relaxation, which causes the number of Fe–Fe near neighbours to increase and thereby M_s to increase; another is the randomizing effect of thermal vibrations, which decreases M_s. On annealing at 300 °C, the former factor is expected to be less than the latter because only a little α-Fe phase occurred; therefore M_s is a little less than that of the as-prepared specimen. On annealing at 400 °C, it is expected that the former factor is equal to or a little larger than the latter factor because more α-Fe phase occurred; so M_s is a little higher than that of the as-prepared specimen. When the annealing temperature is higher than 400 °C, the randomizing effect of thermal vibration is obviously strong; in addition, a non-ferromagnetic phase, a solid solution of Fe in Ni including some boron and phosphorus and t-Fe_3B phase, occurs and increases on increasing the annealing temperature although the amount of α-Fe phase also increases somewhat. Thus, M_s decreases rapidly after annealing at 400 °C.

3.3. Coercivity

Figure 3 shows the Ni content dependence of coercivity H_c for the Fe–Ni–P–B NSAAPs. It can be seen that H_c increases on increasing the Ni content or Fe content for the Fe-based or Ni-based alloys, respectively, which means that there is a maximum for the H_c versus Ni content plot. The present result is similar to that reported by Nafis *et al* [7] for ultrafine Fe–Ni–B particles prepared by chemical reduction. They found that the H_c of Fe–Ni–B particles increased and reached a maximum; it then decreased as the concentration of Ni increased. Nafis *et al* [4] also found that the coercivity of Fe–B particles increased with increasing B content and went through a maximum at a B concentration of around 15 at.%. It should be noted that the coercivity H_c for the liquid-quenched ribbon is much less than that for the powders. In fact, the present results on H_c for the as-prepared Fe–Ni–P–B NSAAPs range from 68 to 223 Oe, compared with about 0.01–0.04 Oe [15] for the $Fe_{40}Ni_{40}P_{14}B_6$ ribbon.

The coercivity depends on the structural inhomogeneities and the magnetic anisotropy of a sample. Even for the same specimen, Luborsky *et al* [25] noted that casting in air resulted in a H_c about two to three times larger than that for casting in vacuum because of the rougher surfaces in the former case. The liquid-quenched samples have better structural homogeneity, which results in a very low value of H_c but the NSAAP samples have an inhomogenous structure, so that their H_c-values are very large. On the other hand, it is usually understood that the origin of coercivity mainly depends on the magnetization reversal which takes place by domain wall motion. For a uniform and perfectly amorphous material such as the liquid-quenched ribbon, domain walls will be unstable, and magnetization reversal proceeds by uniform rotation, starting first in the regions with the weakest anisotropy; therefore, H_c will be very small. However, NSAAPs have ultrafine spherical morphology with a size comparable with a single-domain size [26] and the surface of the NSAAPs is covered with a thin oxide film owing to the high surface

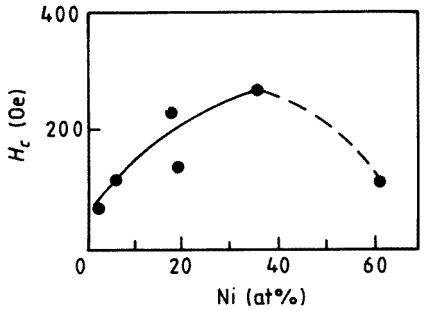

Figure 3. Coercivity H_c of Fe–Ni–P–B NSAAPs as a function of Ni content at room temperature.

reactivity. Therefore, the extrinsic defects such as surface roughness, the presence of surface anisotropy and the surface oxidation layer make the value of H_c in NSAAPs very large.

As for the compositional dependence of H_c for Fe–Ni–P–B NSAAPs, it is easy to understand from their structure and the amount of oxide film covered on the particles. Saida *et al* [26] studied the effect of amorphicity on H_c for Fe–B particles prepared by chemical reduction and found that the Fe–B powder prepared in the vicinity of 293 K appeared to have the best amorphicity; therefore, its H_c was a minimum. The reason is that, the more homogeneous the structure, the lower H_c. As mentioned in section 3.1, the structures for samples 4 and 5 were amorphous plus small crystalline phases, but those for the other four samples were perfectly amorphous. Therefore, H_c for samples 4 and 5 should be larger than for the other samples. On the other hand, our measurements show that the amounts of oxygen for samples 4 and 5 are higher than for the other four samples, which also makes H_c for samples 4 and 5 larger than for the other samples.

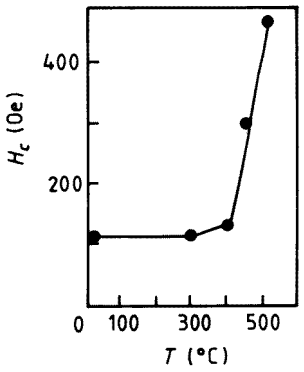

Figure 4. Temperature dependence of H_c for the sample 2 ($Fe_{76.9}Ni_{6.2}P_{2.0}B_{14.9}$).

The dependence of H_c for Fe–Ni–P–B NSAAPs on the annealing temperature was studied. Figure 4 shows the results for specimen 2. It is obvious that H_c is basically constant (from 111 to 133 Oe) when the annealing temperature is lower than 400 °C. The α-Fe phase starts to precipitate from the amorphous matrix but the amount of α-Fe is low, which causes the structure to be somewhat inhomogeneous, thereby making the H_c slightly higher than for the as-prepared sample. For annealing temperatures above 400 °C,

H_c increases sharply. This sharp increase in H_c at higher annealing temperatures results from crystallization of the alloy, which is the same as reported for Fe–B alloy prepared by sputtering [27] and by electroless plating [28].

3.4. Remanence-to-saturation ratio

Figure 5 shows the values of remanence-to-saturation ratio K as a function of P + B content in Fe–Ni–P–B NSAAPs. Obviously, the values are very small, varying from 0.03 to 0.15, which is even less than those (0.21–0.24) of Fe–B amorphous alloys prepared by electroless plating [28]. Ohnuma *et al* [29] studied the remanence-to-saturation ratio for the Fe–B ultrafine metallic particles and found that the value of the ratio was less than 0.2 when the size of the amorphous ultrafine particle association which was composed of a number of finer subparticles of 30–50 nm diameter reached the critical size of a single-domain particle. They argued that this small value of K is qualitatively attributed to the magnetic field which occurs between particles when they approach one another very closely. If the particles approach one another, the magnetic field between particles increases and it decreases the magnetostatic energy of each particle. Thus, the magnetic shape anisotropy becomes large because it originates from the anisotropy of magnetostatic energy of the free pole which appears on the surface of particle and thereby leads to small K-values. Obviously, the present case is similar to this case. In other words, the small K-values for the nanosize particles are caused by their structural imhomogeneities.

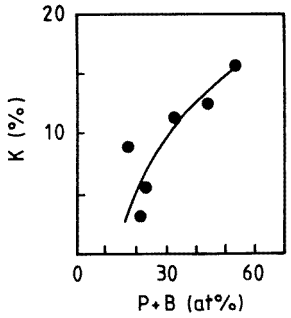

Figure 5. Remanence-to-saturation ratio of K of Fe–Ni–P–B NSAAPs as a function of P + B content at room temperature.

The temperature dependence of K for sample 2 also was studied. The results are shown in figure 6. After annealing from 300 to 500 °C, the values of K are still small (less than 0.15), which means that the powders are still very inhomogeneous even after annealing.

4. Conclusions

Six quaternary Fe–Ni–P–B NSAAPs have been prepared by chemical reduction. The powders have a spherical morphology with a diameter ranging from 20 to 200 nm.

The saturation magnetization of the powders was found to decrease, to go through a minimum and to increase slightly with increasing Ni content and decreasing Fe content. The study on the temperature dependence of M_s indicated that M_s was changed only a little at lower annealing temperatures but decreased sharply for annealing temperatures higher than

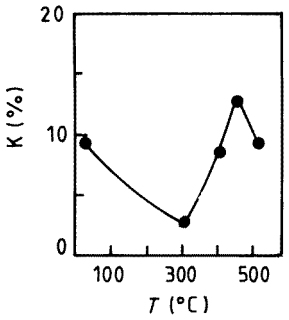

Figure 6. Temperature dependence of K for the sample 2 ($Fe_{76.9}Ni_{6.2}P_{2.0}B_{14.9}$).

400 °C. Using the covalent bonding model and the crystallization products of the sample, these data could be well understood.

The coercivity for the Fe–Ni–P–B NSAAPs was found to increase, to go through a maximum and to decrease with increasing Ni content and decreasing Fe content. The effect of annealing temperature on H_c was that H_c is basically constant at lower annealing temperatures and then increases sharply at temperatures higher than 400 °C.

The remanence-to-saturation ratio was very low, not larger than 0.15; even the powders were annealed at a temperature of 500 °C for 1 h, which indicated that the samples were very inhomogeneous.

Acknowledgments

This research was supported by Development Research Grant 91252032 from the Ministry of Machine Industry of China.

References

[1] van Wonterghem J, Morup S, Charles S W, Wells S and Villadsom J 1985 *Phys. Rev. Lett.* **55** 410
[2] van Wonterghem J, Morup S, Koch C J W, Charles S W and Wells S 1986 *Nature* **322** 622
[3] Luborsky F E, Becker J J, Walter J L and Martin D I 1980 *IEEE Trans. Magn.* **16** 521
[4] Nafis S, Hadjipanayis G C, Sorensen C M and Klabunde K J 1989 *IEEE Trans. Magn.* **25** 3641
[5] Nafis S, Tang Z X, Dale B, Klabunde K J, Sorensen C M and Hadjipanayis G C 1988 *J. Appl. Phys.* **64** 5835
[6] O'Handley R C, Hasegawa R, Ray R and Chou C P 1976 *Appl. Phys. Lett.* **29** 330
[7] Nafis S, Hadjipanayis G C and Sorensen C M 1990 *J. Appl. Phys.* **67** 4478
[8] Yi Ge and Zhang Bangwei 1995 *Proc. 2nd PRICM* ed K S Shin, K Yoon and S J Kim (Seoul: Korean Institute of Metals and Materials) p 1267
[9] Yi Ge, Zhang Bangwei, Wu Lijun and Yang Qiaoqin 1995 *Physica* B **216** 103
[10] Zhang Bangwei and Yi Ge 1996 submitted
[11] Baltz A, Freitag W O, Greifer A P and Suchodolski V 1981 *J. Appl. Phys.* **52** 2456
[12] Watanabe A, Vehori T, Saitoh S and Imaoka Y 1981 *IEEE Trans. Magn.* **17** 1455
[13] Corrias A, Ennas G, Licheri G, Marongin G, Musini A, Paschina G, Piccaluga G, Pinna G and Magini M 1988 *J. Mater. Sci. Lett.* **7** 407
[14] Inoue A, Saida J and Masumoto T 1988 *Metall. Trans.* A **19** 2315
[15] Luborsky F E 1980 *Ferromagnetic Materials* vol 1, ed. E P Wohlfarth (Amsterdam: North-Holland) p 451
[16] Moorjani K and Coey J M D 1984 *Magnetic Glasses* (Amsterdam: Elsevier)
[17] Egami T 1984 *Rep. Prog. Phys.* **47** 1601
[18] de Boer F R, Boom R, Mattens W C M, Miedema A R and Niessen A K 1988 *Cohesion in Metals* (Amsterdam: North-Holland) p 707

[19] Cordts B, Pease D M and Azaroff L V 1980 *Phys. Rev.* B **22** 4692
[20] Joyner D J, Johnso O, Hercules D M, Bullett D W and Weaver J H 1981 *Phys. Rev.* B **24** 3122
[21] Ching W Y 1986 *Phys. Rev.* B **34** 2080
[22] Stadnik Z M and Stroink G 1988 J. Non-Cryst. Solids **99** 233
[23] Corb B W, O'Handley R C and Grant N J 1983 *Phys. Rev.* B **27** 636
[24] Hatta S, Egami T and Graham C D Jr 1978 *Proc. 3rd Int. Conf. on Rapidly Quenched Metals* vol 2, ed B Cantor (London: Metals Society) p 183
[25] Luborsky F E, Leibermann H H, Becker J J and Walter J L 1978 *Proc 3rd Int. Conf. on Rapidly Quenched Metals* vol 2, ed B Cantor (London: Metals Society) p 188
[26] Saida J, Inoue A and Masumoto T 1991 *Metall. Trans.* A **22** 2125
[27] Stobieki F, Dubowik J and Baszynski J 1985 *Proc 5th Int. Conf. on Rapidly Quenched Metals* ed S Steeb and H Warlimont (Amsterdam: North-Holland) p 1211
[28] Zhang Bangwei, Hu Wangyu and Zhu Deqi 1993 *Physica* B **183** 205
[29] Ohnuma S, Nakanouchi Y and Masumoto T 1985 *Proc. 5th Int. Conf. on Rapidly Quenched Metals* ed S Steeb and H Warlimont (Amsterdam: North-Holland) p 1117